Soft Matter

PAPER

View Article Online
View Journal | View Issue

Cite this: *Soft Matter*, 2020, **16**, 2342

Design principles for metamorphic block copolymer assemblies

Alessandro Ianiro, [ab] Steven P. Armes [c] and Remco Tuinier *[ab]

Received 15th November 2019,
Accepted 2nd February 2020

DOI: 10.1039/c9sm02263e

rsc.li/soft-matter-journal

Certain block copolymer assemblies in selective solvents undergo dynamic morphology transitions (metamorphism) on varying the solution temperature. Despite the great application potential, there is a lack of fundamental understanding of the relationship between copolymer composition and the thermally-induced metamorphic behavior. Herein this relationship is studied by applying Scheutjens-Fleer Self-Consistent Field (SF-SCF) theory to develop fundamental design principles for thermoresponsive diblock copolymers exhibiting metamorphic behavior. It is found that metamorphism is caused by variation in the degree of stretching of the lyophobic blocks in response to changes in solvency. An optimal lyophobic/lyophilic block length ratio interval $3.5 \lesssim f_B \lesssim 5.5$ is identified. Such a f_B window allows switching between spheres, cylinders and vesicles as preferred morphologies, with relatively small changes in the lyophobic block solvency. The transition from spheres to cylinders and from cylinders to bilayers can be controlled by varying f_B, the overall degree of polymerization of the diblock copolymer, and by choosing an appropriate lyophilic block. Empirical relationships are provided to establish a connection between the SCF–SCF predictions and experimental observations.

Introduction

When dispersed in selective solvents, block copolymers (BCPs) form supramolecular colloidal structures whose equilibrium characteristics are dictated by the copolymer composition and how each block interacts with the solvent.[1–4] Such self-assembly is spontaneous and is driven by the tendency of the lyophobic block to minimize its contact with the solvent owing to a finite block-solvent interfacial tension (γ). This leads to the formation of structures, where collapsed lyophobic chains and the well-solvated lyophilic chains are segregated into different domains. Various morphologies have been observed experimentally, including spherical micelles, worm-like micelles, vesicles, platelets, and other more complex architectures.[3,5,6] To modulate self-assembly, the copolymer composition (*i.e.*, the relative degrees of polymerization of each block) is usually varied. This is, however, hardly a reversible process. In this context, stimulus-responsive block copolymers[7–9] have been given considerable recent attention because of their rich, versatile and often reversible self-assembly behavior. In some cases, the equilibrium morphology can be switched by using external stimuli such as the solution temperature (*i.e.*, without modifying the copolymer composition).[8,10–13] We refer to such assemblies as metamorphic.

Metamorphic block copolymer assemblies have several potential applications, including drug delivery,[7,8] preparation of thermoreversible hydrogels[10] and as stimuli-responsive oil thickeners.[12] The design of metamorphic assemblies is challenging because the underlying mechanisms regulating the transitions between different copolymer morphologies are only partially understood, particularly in relation to the copolymer (structural and chemical) composition. From an applications perspective, it would be useful to be able to predict metamorphic self-assembly behavior for a given new diblock copolymer in order to avoid extensive trial-and-error investigations.

Numerical self-consistent field computations have been used in the past to study morphology transitions exhibited by self-assembled block copolymer nano-objects. For example, morphology transitions can be induced by changing the size of the solvent molecules,[14] varying the solution temperature[15] or by the addition of nanoparticles when the block copolymer chains are under confinement.[16] Numerical self-consistent field methods are appealing for their low computational cost and, unlike full computer simulations, are suitable for extensive systematic studies using a wide range of parameters. In this work, the metamorphic self-assembly of AB diblock copolymers is studied using Scheutjens-Fleer Self-Consistent Field (SF-SCF) theory.[17,18] This approach is based on Flory–Huggins mean-field theory,[19] but accounts for inhomogeneity and concentration gradients in the system, enabling the formation

[a] *Laboratory of Physical Chemistry, Department of Chemical Engineering and Chemistry, Eindhoven University of Technology, PO Box 513, 5600 MB Eindhoven, The Netherlands. E-mail: r.tuinier@tue.nl*
[b] *Institute for Complex Molecular Systems (ICMS), Eindhoven University of Technology, PO Box 513, 5600 MB Eindhoven, The Netherlands*
[c] *Department of Chemistry, Dainton Building, University of Sheffield, Brook Hill, South Yorkshire, S3 7HF, UK*

of self-assembled structures to be studied. Lattices with different geometries (spherical, cylindrical or planar) can be used to study spherical micelles, worm-like micelles or vesicles in order to determine which morphology is thermodynamically preferred under a given set of conditions (*e.g.*, copolymer composition, solvent, temperature, *etc.*). With this strategy, the evolution in metamorphic assemblies on changing the degree of solvation for the structure-directing block can be examined. Furthermore, relatively short computational times enable systematic studies and provide a detailed structural description of the diblock copolymer nano-objects. This information can be translated into novel design principles for metamorphic BCP self-assembly.

Methods

Modeling approach

Metamorphism can be achieved in several ways, for example by changing the solvent itself,[13] by varying temperature,[10,12] and using light[11,20] (a pH switch can also be used, but this case is not discussed here). Herein we focus on thermally-induced metamorphism. In this case, a change in solvency for at least one of the blocks triggers the (usually) reversible transition between two (or more) morphologies. Such changes can be mapped onto variations of a set of interaction parameters, called Flory–Huggins χ parameters,[19] which are a measure of the compatibility (miscibility) between the individual components in the system. Hence they can be regarded as general indicators for solvency. Conveniently, these χ values are input parameters for the SF-SCF computations.

The SF-SCF approach is based on Flory–Huggins mean-field theory and utilizes numerical lattice computations. This accounts for concentration gradients by means of the Edwards formalism.[21] For each component i in the system, there is a segment potential $u_i(r)$ at each position in the lattice (here r is a coordinate vector indicating the position in the lattice). The normalized probability $P_i(r)$ of finding the component i at the position r is proportional to a Boltzmann factor $e^{-u_i(r)/k_BT}$. The potential at a given position r is influenced by the composition of the adjacent sites, hence it depends on the distribution of segments and molecules, $\varphi_i(r)$. Given this mutual dependence between $\varphi_i(r)$ and $u_i(r)$, an iterative procedure is used to determine the equilibrium segment distribution in order to minimize the free energy of the system.

This problem can be simplified if concentration gradients are considered in one direction only. In this case, the lattice can be envisaged as a collection of layers situated at a distance r from an initial layer. In this configuration, the potential $u_i(r)$ varies only in the direction of r and the normalized probability $P_i(r)$ of finding a certain segment in the lattice layer (r) corresponds to its volume fraction $\varphi_i(r)$ within the layer. The incompressibility ensures that $\sum_i \varphi_i = 1$ for each layer. Further details of the calculation of $u_i[\varphi_i(r)]$ and $\varphi_i[u_i(r)]$ can be found in the original study by Scheutjens and Fleer[18,22] and related publications.[4]

The SF-SCF is a general method to study the phase behaviour of multicomponent systems,[4] as well as interfacial phenomena such as adsorption[23] or depletion.[24] Here we apply this method for the first time to systematically study the metamorphic behaviour of self-assembled block copolymer nano-objects in aqueous solution as a function of the solvency of the water-insoluble structure-directing block.

Thus, the self-assembly of an AB diblock copolymer is studied in a solvent S. The lyophilic A block and the lyophobic B block are composed of N_A and N_B segments, respectively. As the system comprises three components (A, B and S), three pairwise interaction parameters χ_{AS}, χ_{BS}, χ_{AB} need to be specified in the calculations. A full description of the computational set-up is reported below.

Metamorphism is often observed in systems with stimuli-responsive lyophobic blocks. In the SF-SCF computations, metamorphism is induced here by varying the interaction parameter between solvent and the lyophobic block χ_{BS}, which is varied between 0.5 and 2.5. Practically, the interval $0.5 \lesssim \chi_{BS} \lesssim 1.5$ is the most relevant regime for thermoreversible metamorphic behavior, as for $\chi_{BS} \lesssim 0.5$ the copolymer is expected to be always soluble,[19] while for $\chi_{BS} \gtrsim 1.5$ the assemblies are likely to be kinetically frozen, thus losing their ability to switch morphology owing to a vanishing critical aggregation concentration (*i.e.* the concentration of free copolymer chains that are in equilibrium with the assemblies).[25–27] It is emphasized that the SF-SCF computations performed here do not account for kinetic effects – it is not possible to assess the time scales that might be required for the observation of metamorphic behavior.

Lattice and boundary conditions

Numerical SF-SCF lattice computations were performed with the SFbox program provided by Prof. F. A. M. Leermakers (Wageningen University, The Netherlands). The settings of the boundary conditions, the lattice and interaction parameters are described below.

Unless specified, SCF computations were performed on lattices containing L = 200 lattice layers and either spherical, cylindrical or planar geometries to study spherical micelles, cylindrical micelles or vesicles, respectively. It was confirmed that variation of L to larger values did not affect the computed equilibrium properties; no lattice size-related artifacts were observed. A lattice coordination number (z) of 3 was used for each geometry and the lattice constant l (*i.e.* the size of the lattice unit) was set to unity. For a flat geometry, two mirrors are placed at the first and the last lattice sites. For the spherical and cylindrical geometries, a mirror was located at the last lattice layer (with the first layer corresponding to the center of the lattice).

All compounds (the solvent molecule S and the A and B monomer segments) were assumed to occupy a single lattice site. The diblock copolymer chains were assumed to be neutral (uncharged) in character and perfectly homogeneous in chain length (*i.e.* M_w/M_n = 1.00).

Interaction parameters

The system is composed of three components so three pairwise interaction parameters χ (χ_{AS}, χ_{BS}, χ_{AB}) must be specified in the calculations. The parameter χ_{BS} is varied between 0.5 and 2.5 to

simulate changes in the solubility of the lyophobic block in response to the applied stimulus. Several numerical values for χ_{AS} and χ_{AB} were examined; these values are specified each time during the discussion of the results.

Determination of the equilibrium properties of the assemblies

For each copolymer and each set of interaction parameters, the equilibrium self-assembled structure was determined by optimizing the free energy of the (lattice) system of interest with respect to the spatial distribution of each component (concentration profile), and with respect to the copolymer lattice occupancy θ (*i.e.* the number of lattice sites occupied by copolymer molecules in the lattice).[28] This minimization is performed by assuming that only a single self-assembled structure is formed in the lattice. Justification of this protocol has been discussed in the literature.[17,18] At equilibrium, the copolymer chains in the lattice are distributed between bulk solution (θ^{bulk}) and self-assembled structure (θ^{excess}), $\theta = \theta^{excess} + \theta^{bulk}$, as specified by the equilibrium concentration profile. The copolymer bulk concentration (φ_{BCP}^{bulk}) can be expressed as a function of the total lattice volume V:

$$\varphi_{AB}^{bulk} = \frac{\theta^{bulk}}{V}. \quad (1)$$

The parameter φ_{AB}^{bulk} can be interpreted as the critical aggregation concentration of the self-assembled structure. It is noted that V is the total number of sites composing the lattice, and its definition depends on the specific lattice geometry:

$$\begin{aligned} V_{spherical} &= \frac{4}{3}\pi L^3 l^3, \\ V_{cylindrical} &= \pi L^2 l^3, \\ V_{planar} &= L l^3, \end{aligned} \quad (2)$$

where l is the lattice constant. The mean aggregation number N_{agg} of the self-assembled structure is given by

$$N_{agg} = \frac{\theta^{excess}}{N_A + N_B}. \quad (3)$$

For spherical micelles, N_{agg} is the number of copolymer chains forming the micelle; for cylindrical micelles, N_{agg} is the number of copolymer chains contained in a slice of the cylinder with a thickness equal to the lattice constant l; in the flat geometry (which is valid for vesicles) N_{agg} is the number of copolymer chains per unit surface area.

To determine the thermodynamically preferred morphology, the calculations are repeated in lattices with differing geometries (spherical, cylindrical and planar). The copolymer φ_{AB}^{bulk} values are computed for each morphology and then compared. The geometry that has the lowest critical aggregation concentration (φ_{AB}^{bulk}) corresponds to the preferred morphology, since the dimensionless free energy of a copolymer chain within a self-assembled structure (g_{AB}^{sas}) is approximately given by[29]

$$\bar{g}_{AB}^{sas} \approx \ln\left(\frac{\varphi_{AB}^{bulk}}{N}\right). \quad (4)$$

We choose to compare the various φ_{AB}^{bulk} values, rather than the optimized free energies obtained from the computations. This is because φ_{AB}^{bulk} is independent of the lattice size. This allows independent optimization of the lattice size for each lattice geometry, which significantly reduces the computation time.

Calculation of φ_S^{core}, α and ε

The solvent volume fraction in the core φ_S^{core} can be estimated from the solvent equilibrium concentration profile at the center of the insoluble B core. From the values of φ_S^{core} and Nagg the surface area α occupied by each copolymer chain at the core–corona interface can be calculated. For the different lattice symmetries, geometric arguments can be used to show that

$$\bar{\alpha} = \frac{\alpha}{l^2} = \left(\frac{36\pi {N_B}^2}{\left(1-\varphi_S^{core}\right)^2 N_{agg}}\right)^{\frac{1}{3}} \quad (5)$$

for the spherical geometry,

$$\bar{\alpha} = \left(\frac{4\pi N_B}{\left(1-\varphi_S^{core}\right) N_{agg}}\right)^{\frac{1}{2}} \quad (6)$$

for the cylindrical geometry, and

$$\bar{\alpha} = \frac{2}{N_{agg}} \quad (7)$$

for the planar geometry.

In principle, the end-to-end distance of the B blocks, ε, could be determined by the concentration profiles from the thickness of the B core. In practice, the existence of a wide interface (Fig. 4) makes it difficult to formally define the boundary of the core region. Therefore, we have also derived the following expressions for:

$$\bar{\varepsilon} = \frac{\varepsilon}{l} = \frac{3N_B}{\alpha\left(1-\varphi_S^{core}\right)} \quad (8)$$

for the spherical geometry,

$$\bar{\varepsilon} = \frac{2N_B}{\alpha\left(1-\varphi_S^{core}\right)} \quad (9)$$

for the cylindrical geometry, and

$$\bar{\varepsilon} = \frac{N_B}{\alpha\left(1-\varphi_S^{core}\right)} \quad (10)$$

for the planar geometry. These geometrical definitions of $\bar{\alpha}$ and $\bar{\varepsilon}$ imply that the molecular packing parameters[30] of the assemblies, are $P \equiv 1/3$ for the spherical morphology, $P \equiv 1/2$ for the cylindrical morphology and $P \equiv 1$ for the bilayer (vesicle) morphology.

Determination of χ_{SP} from φ_S^P

The SCF computations have been used to derive an empirical relationship that allows the polymer–solvent interaction parameter χ_{SP} to be determined for an insoluble homopolymer P in a solvent S. According to this method, χ_{SP} can be evaluated by measuring the volume fraction φ_S^P of S taken up by P when

these two species are in contact. This can be achieved gravimetrically by using a microbalance if the density of the homopolymer and the solvent are known.

SF-SCF calculations have been used to compute equilibrium concentration profiles for homopolymer-solvent systems for a planar geometry ($L = 100$, $l = 1$) as a function of χ_{SP} in the range $0.5 \leq \chi_{SP} < 2$. Various homopolymers (P), with $100 \leq N_P \leq 800$, have been simulated. A total polymer volume fraction in the lattice $\varphi_P = 0.1$ was used for each computation. For $\chi_{SP} \gtrsim 0.7$ phase separation into P-rich and S-rich phases is predicted. The solvent concentration in the P-rich phase, φ_S^P, is fitted with χ_{SP} to provide the empirical relationship shown in eqn (11) (in Results and discussion).

Results and discussion

SCF results

The SF-SCF computations have been first performed to evaluate the preferred morphology of AB diblock copolymers with $N_A = 50$ and various relative block lengths $f_B = N_B/N_A$. The calculations are performed assuming $\chi_{AS} = 0.4$ and $\chi_{AB} = 1$, corresponding to a moderately soluble A block, well segregated from the B block. The results are summarized in a phase diagram (Fig. 1a) that reveals an optimal f_B window ($3.5 \lesssim f_B \lesssim 5.5$ for the selected parameters), where several possible (di)block copolymer morphologies can be obtained within a reasonably narrow χ_{BS} range. Outside of this f_B interval, only one ($f_B \lesssim 2$) or two ($2 \lesssim f_B \lesssim 3$, $f_B \gtrsim 5.5$) morphologies are predicted for $0.5 \lesssim \chi_{BS} \lesssim 2.5$.

The χ_{BS} values marking the sphere-to-cylinder ($\chi_{BS}^{S\to C}$) and cylinder-to-bilayer ($\chi_{BS}^{C\to B}$) transitions are also influenced by the total copolymer chain length $N = N_A + N_B$ (Fig. 1b). As shown in Fig. 1b, $\chi_{BS}^{S\to C}$ is only weakly dependent on N, while a marked, linear $\chi_{BS}^{C\to B}$ increase is observed when increasing N at a fixed f_B value of 4. When increasing the overall copolymer chain length, the stability windows for the various morphologies become wider (Fig. 1b).

Together with the preferred morphology, the SF-SCF computations provide structural information, such as the mean aggregation number Nagg and the amount of solvent present in the core of the self-assembled structure φ_S^{core} (see Methods for further details). These quantities can be used to estimate the average end-to-end distance of the lyophobic B block (ε) and the area that each copolymer chain occupies at the core–corona interface (α). The calculations for ε and α are described in Methods. The χ_{BS}dependence of these quantities, illustrated in Fig. 2 for A_{50}-B_{200} ($f_B = 4$, $\chi_{AS} = 0.4$, $\chi_{AB} = 1$), provide a molecular-level interpretation of the metamorphic behaviour. Increasing χ_{BS} causes a reduction in compatibility between B and S, which in turn drives the expulsion of solvent from the nano-objects (Fig. 2a); this is in agreement with previous experimental studies of self-assembled diblock copolymer nano-objects.[10,31] As a result, the copolymer chains come into closer proximity (increasing the aggregation number with a consequent reduction in α, Fig. 2b) and are forced to stretch (increase in ε, see Fig. 2c). Such chain stretching triggers the morphology transition. The equilibrium morphology adopted is determined by the balance between interfacial energy ($\Delta g^{interface} = \gamma\alpha$), core elastic energy ($\Delta g^{core}$) and corona elastic energy[32,33] (Δg^{corona}).

Core and corona elastic energies are entropic contributions. They account for variation in the configurational entropy caused by perturbations of the core (ε) and corona (δ) end-to-end distances (Fig. 2d). For a fixed α value, $\Delta g^{interface}$ is morphology-independent and the preferred morphology is dictated by the balance between Δg^{corona} and Δg^{core}. The spherical morphology is associated with the lowest Δg^{corona} but the highest Δg^{core} (Fig. 2d). Conversely, bilayer morphologies such as vesicles exhibit the highest Δg^{corona} but the lowest Δg^{core}. Therefore, an increase in ε modifies the energetic balance between any given pair of

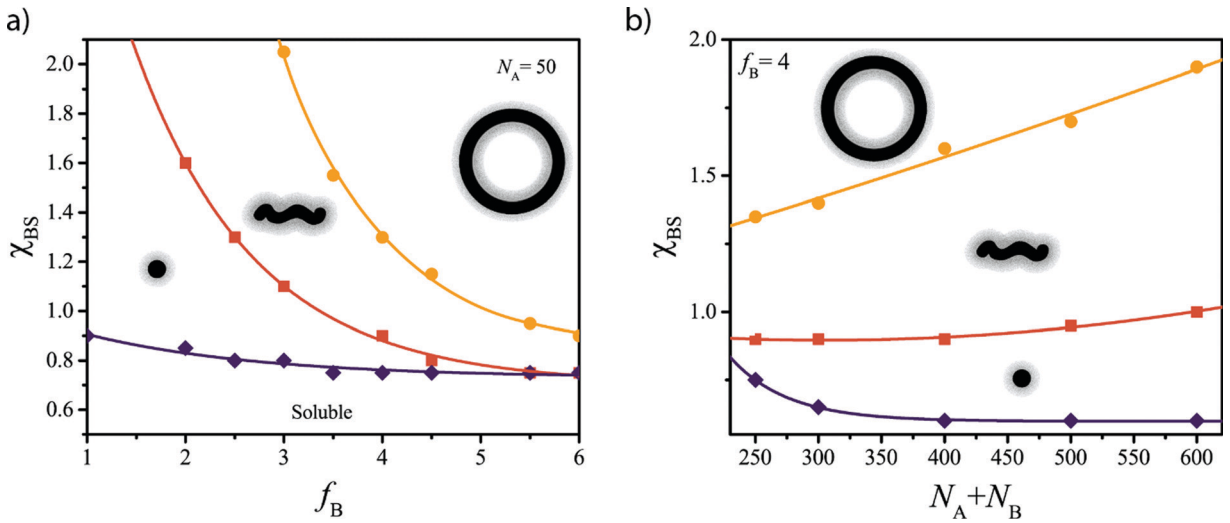

Fig. 1 SF-SCF equilibrium morphology diagrams, displaying the preferred morphology as a function of the lyophobic block solubility χ_{BS} for (a) diblock copolymers with different relative block lengths $f_B = N_B/N_A$ ($N_A = 50$, $\chi_{AS} = 0.4$ and $\chi_{AB} = 1$) and (b) copolymers with fixed $f_B = 4$ and different total copolymer chain lengths N($\chi_{AS} = 0.4$ and $\chi_{AB} = 1$). The markers represent the SF-SCF data; the curves serve as a guide to the eye.

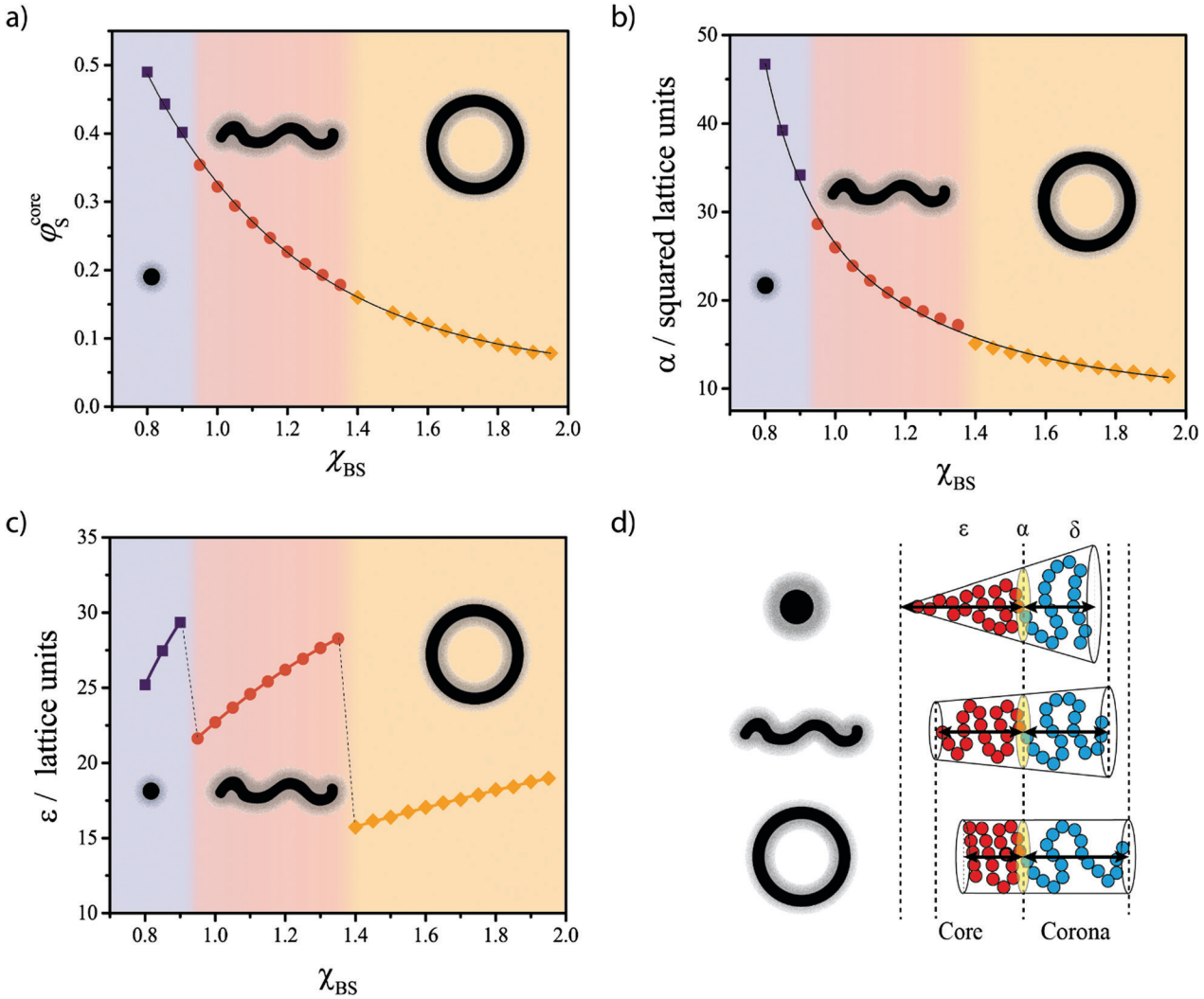

Fig. 2 (a) Solvent volume fraction in the lyophobic core of the block copolymer assemblies φ_S^{core}, (b) dimensionless surface area $\bar{\varepsilon}$ occupied by each polymer at the core–corona interface, and (c) dimensionless end-to-end distance of the lyophobic block $\bar{\varepsilon}$ for A_{50}-B_{200} (χ_{AB} = 1, χ_{AS} = 0.4) as a function of the interaction parameter between the solvent and the lyophobic block χ_{BS}. The stability regions for the different copolymer morphologies are denoted by the differing background colors. The schematic representation in (d) illustrates the changes in the end-to-end distances calculated for the lyophilic (δ) and lyophobic (ε) chains associated with the morphology transitions for a fixed α value.

assemblies, thus driving the morphology transition (first to cylindrical, then to bilayer morphology). Each transition is accompanied by a steep reduction in ε (Fig. 2c) at the expense of an increasing δ (Fig. 2d).

In contrast, lower χ_{AB} values (which correspond to greater inter-block compatibility) are associated with a reduction in $\chi_{BS}^{S\to C}$ and $\chi_{BS}^{C\to B}$ because the lyophilic chains are partially embedded at the core–corona interface (Fig. 4) and hence screen the cores from the solvent to some extent. As χ_{AB} is reduced, contact between the A and B blocks becomes more favorable and the core screening more effective. This leads to a broader core–corona interface, as indicated by the concentration profiles shown in Fig. 4. Entrapment of more A segments through the interface can be interpreted as an effective reduction in the corona chain length, with the consequent increase in f_B shifting the morphology transitions towards lower χ_{BS} values (Fig. 1a). These results suggest that the choice of the particular lyophilic block can strongly influence the metamorphic behavior.

The effect of varying the lyophilic block solubility (χ_{AS}) and the degree of compatibility between A and B (χ_{AS}) was also investigated. A reduction in χ_{AS} (increase in solubility) leads to expansion of the corona chains because the effective excluded volume of the segments in the A block increases.[18,34] As a result, the energy penalty associated with stretching these lyophilic chains is lower. This affects the balance between Δg^{corona} and Δg^{core}, which in turn shifts the morphology transitions towards higher χ_{BS} values (Fig. 3a).

Translating the SF-SCF results into design principles

As discussed above, SF-SCF theory can be used to guide the design of new experimental systems that exhibit the desired metamorphic behavior. It appears that a composition window (expressed in terms of the relative block length) of $3.5 \lesssim f_B \lesssim 5.5$ is optimal

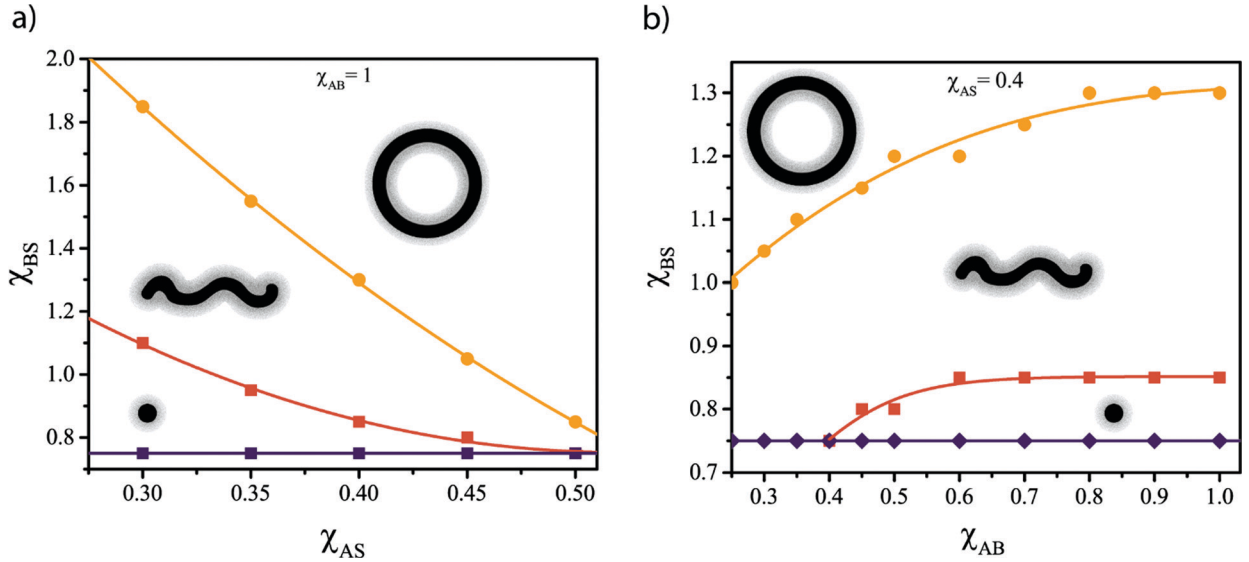

Fig. 3 SF-SCF equilibrium morphology diagrams, displaying the preferred morphology as a function of the lyophobic block solubility χ_{BS} for (a) copolymers with differing lyophilic block solubilities χ_{AS} (N_A = 50, N_B = 200 and χ_{AB} = 1) and (b) copolymers with differing inter-block compatibilities χ_{AB} (N_A = 50, N_B = 200 and χ_{AS} = 0.4).

as the resulting assemblies exhibit metamorphic behavior within a useful χ_{BS} range. This agrees with recent experimental results,[31,35] where two types of block copolymers with temperature-responsive lyophobic blocks and $4.5 \lesssim f_B \lesssim 5$ exhibited the ability to form spheres, cylinders or vesicles in water depending on the solution temperature. The values of $\chi_{BS}^{S\to C}$ and $\chi_{BS}^{C\to B}$ can be controlled by varying f_B and adjusted by an appropriate choice of the lyophilic block (Fig. 3a) and the overall degree of polymerization of the diblock copolymer chains (Fig. 1b). As a result, this optimal window is expected to shift towards higher f_B values when increasing the overall block copolymer length and χ_{AB}, and also when decreasing χ_{AS} (and *vice versa*).

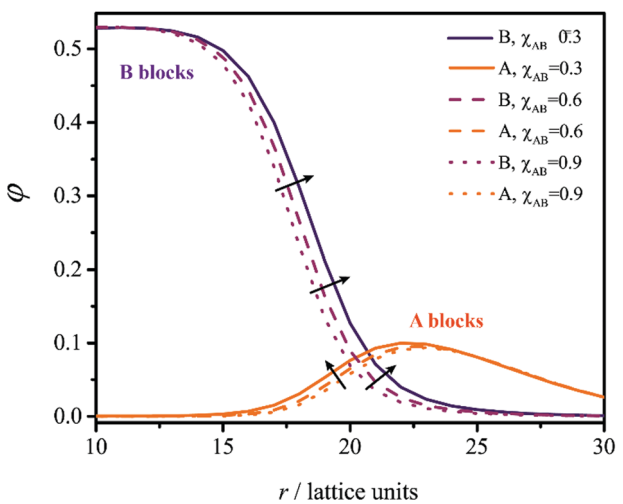

Fig. 4 Equilibrium concentration profiles of A and B segments, showing the spatial distribution of the lyophilic (orange) and lyophobic (purple) blocks as a function of the distance r from the center of A_{50}-B_{200} cylindrical micelles (χ_{BS} = 0.9, χ_{AS} = 0.4) for various inter-block compatibilities χ_{AB}. Arrows indicate the effect of increasing the χ parameters.

The most important aspect of the design of metamorphic assemblies is to evaluate how χ_{BS} depends on the applied stimulus. There are various ways to determine χ parameters[36] but many of them are only valid for soluble polymers and are typically time-intensive measurements requiring specific equipment.[36] For insoluble homopolymers, there is a relationship between χ and the amount of solvent taken up at equilibrium (φ_S^P), as described by Flory–Huggins solution theory.[19] Unfortunately, this relationship cannot be expressed in terms of an exact analytical solution. However, an empirical relation can be derived using numerical analysis or SF-SCF computations (see Methods). Here values of φ_S^P are computed using SF-SCF for a polymer P as a function of the polymer–solvent interaction parameter χ_{SP} for various mean degrees of polymerization, NP.

According to Fig. 5, φ_S^P is chain length-independent, and fitting this data set provides the following approximate empirical relationship:

$$\chi_{SP} \approx \frac{0.56}{(\varphi_S^P)^{\frac{1}{2}}}. \quad (11)$$

Using (11), a numerical value for χ_{BS} and its dependence on the applied stimulus can be readily determined by measuring the solvent uptake (φ_S^P) for a homopolymer with the same composition as the lyophobic block. In principle, this can be achieved simply by gravimetry using a precision microbalance.

It is emphasized that the SF-SCF relative block length f_B does not always correspond to the actual experimental block length ratio. Within the lattice-based SF-SCF theory, all segments have the same size and flexibility, which is not necessarily true in reality. For flexible linear diblock copolymers, one strategy is to compute the ratio between the volumes of the B (V_B). and A (V_A) monomers, $\nu = V_B/V_A$ (the monomer volume can be calculated as the monomer mass divided by the block density).

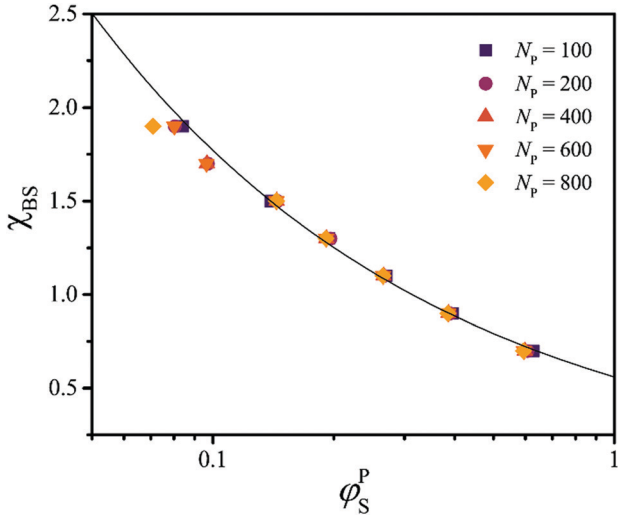

Fig. 5 SF-SCF results (markers) for the relationship between the polymer–solvent interaction parameter χ_{SP} and the solvent volume fraction in the polymer φ_S^P for various homopolymers of differing degrees of polymerization, NP. The full curve represents the empirical fit obtained using eqn (11).

The parameter ν can be multiplied by the experimental block length ratio f_B to obtain an effective parameter ($f_B^{eff} = \nu f_B$), which is an appropriate and reliable reference for interpreting the SF-SCF predictions. Alternatively, one can map the copolymer onto a lattice by considering the actual chain flexibility of each block, which in principle can be evaluated *via* scattering experiments.[37]

Finally, when designing a suitable metamorphic system, it is important to bear in mind that copolymer dispersions might undergo liquid–liquid phase separation under certain conditions.[38] Such phase separation can be minimized by ensuring high inter-block segregation (high χ_{AB}) and choosing highly soluble (low χ_{AS}) lyophilic blocks.[38]

The principles summarized above can be combined with the SF-SCF results to guide the design of metamorphic assemblies, thus avoiding laborious trial-and-error experimentation.

Conclusions

Scheutjens-Fleer Self-Consistent Field (SF-SCF) numerical lattice computations have been used to systematically study diblock copolymer assemblies that undergo thermally-induced metamorphism, *i.e.* reversible morphology transitions between spherical micelles, cylindrical micelles, and bilayers (vesicles). It is found that metamorphism is caused by variation in the degree of stretching of the lyophobic blocks in response to changes in solvency. However, such metamorphism is only observed over a relatively narrow block composition interval. The most relevant composition range appears to be $3.5 \lesssim f_B \lesssim 5.5$, where f_B is the lyophobic/lyophilic block length ratio. The transition from spheres to cylinders and from cylinders to bilayers (and in turn the optimal f_B window), can be controlled by varying the overall degree of polymerization of the diblock copolymer chains and also by choosing an appropriate lyophilic block. Empirical relationships are established to connect the SCF–SCF predictions to experimental observations. This study provides a complete theoretical framework for the rational design of AB diblock copolymers that exhibit metamorphic self-assembly behaviour.

Conflicts of interest

There are no conflicts to declare.

Notes and references

1 D. J. Adams, C. Kitchen, S. Adams, S. Furzeland, D. Atkins, P. Schuetz, C. M. Fernyhough, N. Tzokova, J. A. Ryan and M. F. Butler, *Soft Matter*, 2009, **5**, 3086–3096.
2 Z. Zhou, Z. Li, Y. Ren, M. A. Hillmyer and T. P. Lodge, *J. Am. Chem. Soc.*, 2003, **125**, 10182–10183.
3 Y. Mai and A. Eisenberg, *Chem. Soc. Rev.*, 2012, **41**, 5969–5985.
4 F. Leermakers, J. C. Eriksson and H. Lyklema, *Fundamentals of Interface and Colloid Science – Vol. V*, Academic Press, 2005, pp. 4.1–4.123.
5 S. J. Holder and N. A. J. M. Sommerdijk, *Polym. Chem.*, 2011, **2**, 1018–1028.
6 A. Blanazs, S. P. Armes and A. J. Ryan, *Macromol. Rapid Commun.*, 2009, **30**, 267–277.
7 Q. Zhou, L. Zhang, T. H. Yang and H. Wu, *Int. J. Nanomed.*, 2018, **13**, 2921–2942.
8 X. Hu, Y. Zhang, Z. Xie, X. Jing, A. Bellotti and Z. Gu, *Biomacromolecules*, 2017, **18**, 649–673.
9 M. A. Cohen Stuart, W. T. S. Huck, J. Genzer, M. Müller, C. Ober, M. Stamm, G. B. Sukhorukov, I. Szleifer, V. V. Tsukruk, M. Urban, F. Winnik, S. Zauscher, I. Luzinov and S. Minko, *Nat. Mater.*, 2010, **9**, 101–113.
10 S. P. Armes, R. Verber, A. Blanazs, C. W. I. Douglas, A. J. Ryan, J. Z. Heath and O. O. Mykhaylyk, *J. Am. Chem. Soc.*, 2012, **134**, 9741–9748.
11 E. Blasco, J. L. Serrano, M. Piñol and L. Oriol, *Macromolecules*, 2013, **46**, 5951–5960.
12 M. J. Derry, O. O. Mykhaylyk and S. P. Armes, *Angew. Chem., Int. Ed.*, 2017, **56**, 1746–1750.
13 Y. Yu, L. Zhang and A. Eisenberg, *Macromolecules*, 1998, **31**, 1144–1154.
14 W. Li and W. Jiang, *Macromol. Theory Simul.*, 2009, **18**, 434–440.
15 A. M. Rumyantsev, F. A. M. Leermakers, E. B. Zhulina, I. I. Potemkin and O. V. Borisov, *Langmuir*, 2019, **35**, 2680–2691.
16 Q. Pan, C. Tong and Y. Zhu, *ACS Nano*, 2011, **5**, 123–128.
17 P. N. Hurter, J. M. H. M. Scheutjens and T. A. Hatton, *Macromolecules*, 1993, **26**, 5592–5601.
18 G. J. Fleer, M. A. Cohen Stuart, J. M. H. M. Scheutjens, T. Cosgrove and B. Vincent, *Polymers at Interfaces*, Springer, Netherlands, 1993.
19 P. J. Flory, *Principles of Polymer Chemistry*, Cornell University Press, Ithaca, United States, 1953.

20 Y. Zhao, *J. Mater. Chem.*, 2009, **19**, 4887–4895.
21 S. F. Edwards, *Proc. Phys. Soc.*, 1965, **85**, 613–624.
22 J. M. H. M. Scheutjens and G. J. Fleer, *J. Phys. Chem.*, 1979, **83**, 1619–1635.
23 G. J. Fleer, *Adv. Colloid Interface Sci.*, 2010, **159**, 99–116.
24 G. J. Fleer, A. M. Skvortsov and R. Tuinier, *Macromolecules*, 2003, **36**, 7857–7872.
25 S. Choi, F. S. Bates and T. P. Lodge, *Macromolecules*, 2011, **44**, 3594–3604.
26 J. Lu, F. S. Bates and T. P. Lodge, *Macromolecules*, 2015, **48**, 2667–2676.
27 S. Choi, T. P. Lodge and F. S. Bates, *Phys. Rev. Lett.*, 2010, **104**, 047802.
28 T. L. Hill, *J. Chem. Phys.*, 1962, **36**, 3182–3197.
29 H.-J. Butt, K. Graf and M. Kappl, *Physics and Chemistry of Interfaces*, Wiley-VCH Verlag GmbH & Co. KGaA, 2006.
30 J. N. Israelachvili, D. J. Mitchell and W. B. Ninham, *J. Chem. Soc., Faraday Trans. 2*, 1975, 1525–1568.
31 L. P. D. Ratcliffe, M. J. Derry, A. Ianiro, R. Tuinier and S. P. Armes, *Angew. Chem., Int. Ed.*, 2019, **58**, 18964–18970.
32 E. B. Zhulina, M. Adam, I. Larue, S. S. Sheiko and M. Rubinstein, *Macromolecules*, 2005, **38**, 5330–5351.
33 E. B. Zhulina and O. V. Borisov, *Macromolecules*, 2012, **45**, 4429–4440.
34 J. Lyklema, *Fundamentals of Interface and Colloid Science volume V*, Elsevier B.V., Amsterdam, 2005.
35 S. J. Byard, C. T. O'Brien, M. J. Derry, M. Williams, O. O. Mykhaylyk, A. Blanazs and S. P. Armes, *Chem. Sci.*, 2020, **11**, 396–402.
36 J. Brandrup, E. H. Immergut and E. A. Grulke, *Polymer Handbook*, ed. A. Abe and D. R. Bloch, John Wiley and Sons, 4th edn, 2005.
37 H. Morawetz, *Light scattering from polymer solutions*, Academic Press Inc., London, 1973.
38 A. Ianiro, H. Wu, M. M. J. van Rijt, M. P. Vena, A. D. A. Keizer, A. C. C. Esteves, R. Tuinier, H. Friedrich, N. A. J. M. Sommerdijk and J. P. Patterson, *Nat. Chem.*, 2019, **11**, 320–328.